

# SADDLE ANTENNA RF ION SOURCES FOR EFFICIENT POSITIVE AND NEGATIVE IONS PRODUCTION\*

V. Dudnikov<sup>#</sup>, R. Johnson, Muons, Inc., Batavia, IL 60510, USA  
 S. Murrey, B. Han, T. R. Pinnisi, C. Piller, M. Santana, M. Stockli,  
 R. Welton, ORNL, Oak Ridge, TN 37831, USA  
 J. Breitschopf, Taxes Lutheran University, Seguin, TX 78155, USA  
 G. Dudnikova, UMD, College Park, MD 32611, USA

## Abstract

Existing RF Ion Sources for accelerators have specific efficiencies for  $H^+$  and  $H^-$  ion generation  $\sim 3\text{--}5\text{ mA/cm}^2\text{ kW}$ , where about 50 kW of RF power is typically needed for 50 mA beam current production. The Saddle Antenna (SA) SPS described here was developed to improve  $H^-$  ion production efficiency, reliability and availability. In SA RF ion source the efficiency of positive ion generation in the plasma has been improved to 200 mA/cm<sup>2</sup> kW. After cesiation, the current of negative ions to the collector was increased from 1 mA to 10 mA with RF power  $\sim 1.5\text{ kW}$  in the plasma (6 mm diameter emission aperture) and up to 30 mA with  $\sim 4\text{ kW}$  RF. Continuous wave (CW) operation of the SA SPS has been tested on the test stand. The general design of the CW SA SPS is based on the pulsed version. Some modifications were made to improve the cooling and cesiation stability. CW operation with negative ion extraction was tested with RF power up to  $\sim 1.2\text{ kW}$  in the plasma with production up to  $I_c=7\text{ mA}$ . Long term operation was tested with  $\sim 0.8\text{ kW}$  in the plasma with production of  $I_c=5\text{ mA}$ ,  $I_{ex}\sim 15\text{ mA}$ .

A stable long time generation of  $H^-$  beam without degradation was demonstrated in RF discharge with AlN discharge chamber.

## INTRODUCTION

Development of the saddle antenna RF surface plasma source (SA RF SPS) was proposed for improve efficiency of  $H^-$  ion production and improve SPS reliability and availability [1-6]. RF SPS for accelerators have the efficiency of  $H^-$  ion generation  $\sim 1\text{ mA/kW}$  and RF power  $\sim 50\text{ kW}$  is needed for 50 mA beam current production [7-8]. The high RF power required for the sources as well as triggering of the pulsed discharge can create problems for very long term operation. In tested version of SA RF SPS the specific efficiency of positive ion generation was increased to  $\sim 200\text{ mA/cm}^2\text{ kW}$  and a specific efficiency of  $H^-$  production was increased up to  $\sim 20\text{ mA/cm}^2\text{ kW}$  from previous  $\sim 2.5\text{ mA/cm}^2\text{ kW}$ .

The total efficiency of the surface plasma produced fraction of the  $H^-$  beam is a product of the probability of secondary emission of  $H^-$  caused by plasma bombardment of the collar surface around the emission aperture, the probability of extraction of emitted  $H^-$ , and the rate of

bombarding plasma flux [9-12]. The coefficient of secondary emission of  $H^-$  is determined by surface properties (proper cesiation) and the spectrum of the plasma particles bombarding the collar surface around the emission aperture.

The cesiation was improved recently [7] and appears to be nearly optimal. The probability of extraction of  $H^-$  emitted from the collar surface is dependent on the surface collar shape [9-11], which was optimized recently to improve  $H^-$  emission [6]. The problem of efficient plasma generation is being addressed by the development of new RF plasma generators with higher plasma generation efficiency and better concentration of useful plasma flux onto the internal surfaces of the collar around the emission aperture for lower RF power [1-6]. In this project, we use the saddle antenna, which has its RF magnetic field transverse to the source axis, combined with an axial DC magnetic field, to concentrate the plasma on the collar where the negative ions are formed by secondary emission [1-6, 9-11].

## SA SPS DESIGN

The schematic of a large RF SA SPS with the AlN ceramic discharge chamber, saddle antenna, and DC solenoid is shown in Fig. 1. The chamber has an ID=68 mm. The saddle antenna in this SPS with inductance  $L=3.5\text{ }\mu\text{H}$  is made from water cooled copper tube. RF assisted triggering plasma gun (TPG) is attached to discharge chamber from left. An extraction system is attached from right side.

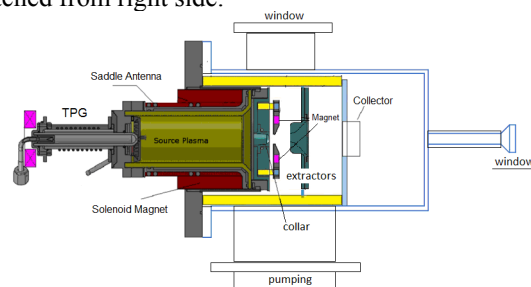


Figure 1: A schematic of the SA SPS with an extraction system and a collector.

A schematic of the extraction system is shown in Fig. 2. The strong transverse magnetic field (up to 1 kG) is created in the collar by permanent magnets (arrows) inserted into water cooled extractor attached to the plasma plate through ceramic insulators.

The schematic of ion beam formation is shown in Fig. 2. Ions extracted from the cone by extraction voltage  $U_{ex}$  between the cone and the extractor and accelerated by voltage in the second gape. Co-extracted electrons are well collected to the extractor along magnetic field lines without drift in crossed  $ExB$  field. The strong transverse magnetic field  $B_t$  suppress electron collection by collector and the secondary emission is suppressed by magnets attached to the collector.

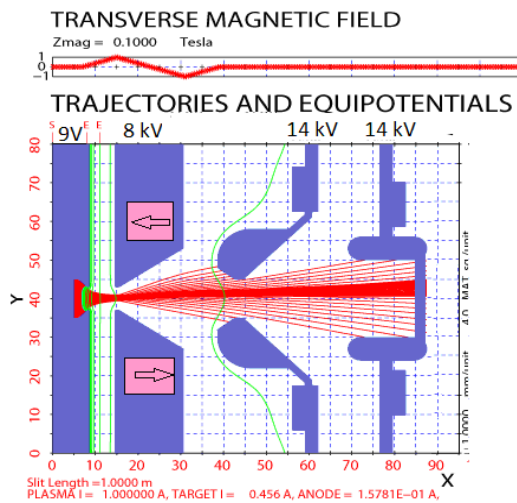


Figure 2: A schematic of ion beam extraction with simulation by PBGUNS (emission aperture is 6 mm). Transverse magnetic field distribution on top.

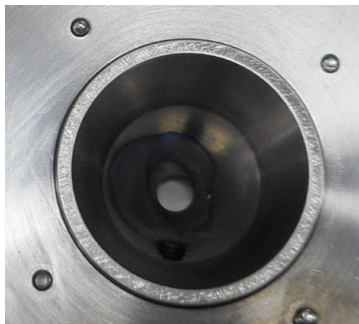


Figure 3: Internal surface of conical collar with autograph of plasma bombardment.

The evidence of this plasma flux behavior is the trace of the dark film deposited on the conical collar surface shown in Fig. 3.

Extractor, accelerator electrode and collector were biased by high voltages  $U_{ex}$  and  $U_c$ . Pulsed currents to these electrodes were registered by Pearson transformers with sensitivity 1 V/A. The magnetic field  $B_t$  up to 250 G was created by solenoid excited by current  $I_m$  up to 70 A with voltage  $U_m$  up to 8 V. A photo of positive ion beam extraction and collector heating by the beam is shown in Fig. 4.



Figure 4: Photo of positive ion beam extraction and collector heating by the beam. Plasma light from emission aperture is visible at a right side. Collector is heated by ion beam up to high temperature ( $\sim 1000^\circ\text{C}$ ).

The photo of  $\text{H}^+$  beam extraction and collector heating by the beam is shown in Fig. 5. The RF discharge in the TPG was excited by RF (13.56 MHz) generator with power up to 0.6 kW. For the SA discharge excitation was used RF (13.56 MHz) generator with power up to 5.5 kW. The RF power loss in SA and matching network was  $\sim 1$  kW and up to  $\sim 4.5$  kW can be used for plasma generation. A Hydrogen gas flow was controlled by MKS mass flow controller.

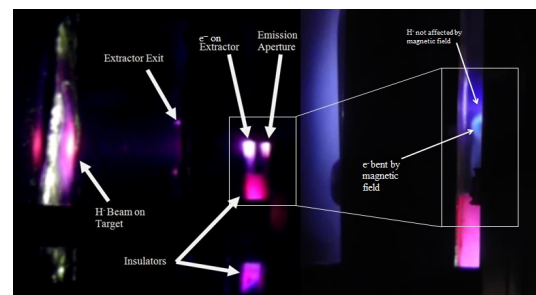


Figure 5: Photo of  $\text{H}^+$  beam extraction and collector heating by the beam. Light from emission aperture is visible at a right site and co-extracted electrons a heating the extractor surface up to high temperature ( $\sim 1000^\circ\text{C}$ ). Collector is heated by ion beam up to high temperature (yellow color). Ceramic insulators luminescent are excited by electron bombardment.

## EXPERIMENTAL RESULTS

Several versions of plasma generators with different antennas and magnetic field configurations were fabricated and tested in the test stand. A pulsed RF (13.56 MHz) discharges with duration 1-2 ms, up to 160Hz and power up to 1.5 kW in the plasma were tested. A signals of positive ion on the collector is shown in Fig. 6. After cesiaion the negative ion current to the collector  $I_c$  was increased from 1 mA to 10 mA and electron current to the extractor  $I_{ex}$  was reduced from 0.15 A to 0.1 A.

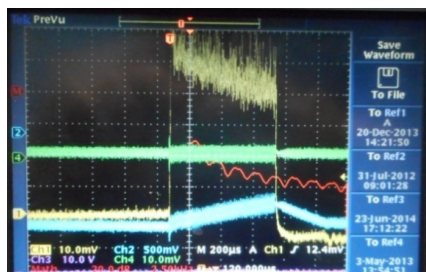


Figure. 6: Signals of positive ion on collector -  $I_c = 50$  mA (Ch1; 10 mA/div) at RF power  $\sim 1.5$  kW in the plasma and a signal of extraction voltage drop (Ch2; 5 kV/div). Time scale is 0.2 ms/div.

Examples of  $I_c$  and  $I_{ex}$  signals are shown in Fig. 7. Dependences of  $I_c$  on RF power in the plasma  $P_{rf}$  is shown in Fig. 8 (upper scale). Dependences of  $I_c$  on the solenoid voltage  $U_m$  is shown in Fig. 9. The collector current  $I_c$  increases by a factor of 7 as the longitudinal magnetic field  $B_l$  increases from 0 to 250 G and increases with the extraction voltage. The accelerator electrode and collector was biased to  $U_c \sim 10$  kV. SA SPS can operate at the gas flow decreased down to  $Q = 4-5$  sccm (standard  $\text{cm}^3/\text{minute}$ ), while the  $\text{H}^+$  current increased up to 10 mA at  $P_{rf} = 1.5$  kW ( $\text{H}^+$  generation efficiency was up to  $I_c/P_{rf} \sim 7$  mA/kW,  $I_c = 30$  mA at  $P_{rf} = 4$  kW with cesiation). More efficient and stable cesiation was produced with a dark film deposition on the emitter cone (2) in Fig. 2.

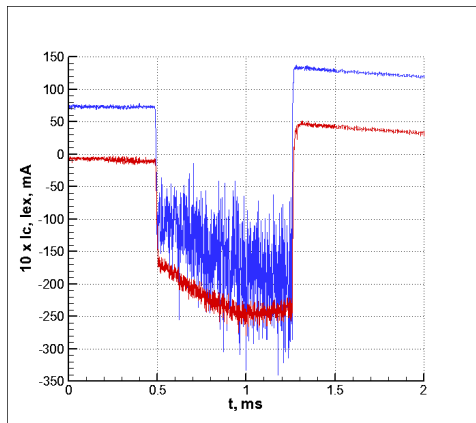


Figure 7: Collector current (red)  $I_c = 30$  mA and extractor current (blue)  $I_{ex} \sim 0.2$  A with RF power  $P_p \sim 4$  kW in the plasma.

Extraction current has a significant level of noise with frequencies  $f_n \sim 1-2$  MHz. Continuous wave (CW) operation of the SA SPS has been tested in the small SNS test stand. The general design of the CW SA SPS is based on the pulsed version considered above [3, 4].

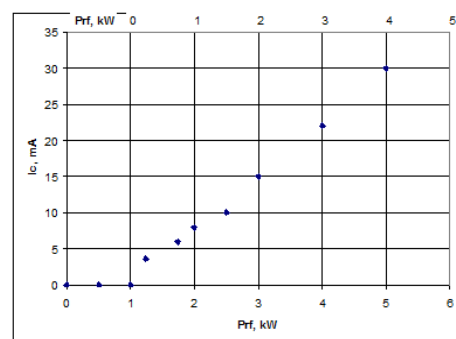


Figure 8: Dependence of the collector current  $I_c$  on RF generator power  $P_{rf}$  (low scale) and RF power in plasma (upper scale) with RF generator Apex 5513.

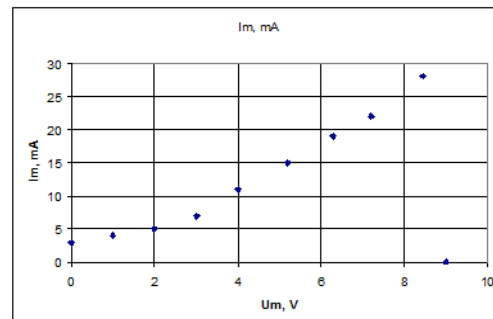


Figure 9: Dependence of  $I_c$  on the solenoid voltage  $U_m$ . RF power in the plasma  $P_{rf} = 4$  kW, extraction voltage 11 kV. Gas flow  $Q = 7.6$  sccm

Some modifications were made to improve cooling and cesiation stability. CW operation of the SA SPS with negative ion extraction was tested with RF power up to  $\sim 1.8$  kW from generator ( $\sim 1.2$  kW in the plasma) with production up to  $I_c = 7$  mA.

## REFERENCES

- [1] V. Dudnikov et al., AIP Conf. Proc. 925, edited by M. Stockli, 153-163 (2007).
- [2] V. Dudnikov et al., THPS026, Proceedings of IPAC2011, San Sebastián, Spain (2011).
- [3] V. Dudnikov et al., Rev. Sci. Instrum. 83, 02A712 (2012).
- [4] V. Dudnikov et al., AIP Conf. Proc. 1390, 411 (2011).
- [5] V. Dudnikov et al., AIP Conf. Proc. 1515, 456 (2013).
- [6] V. Dudnikov et al., AIP Conf. Proc. 1655, 070003 (2015).
- [7] R. F. Welton et al., Rev. Sci. Instrum. 83, 02A725 (2012).
- [8] J. Lettry et al., AIP Conf. Proc. 1515, 302 (2013).
- [9] V. Dudnikov, Rev. Sci. Instrum., 83, 02A708 (2012).
- [10] Yu. I. Belchenko, G. I. Dimov, and V. G. Dudnikov, Nuclear Fusion, 14(1), 113-114 (1974).
- [11] Y. I. Belchenko, G. I. Dimov, and V. G. Dudnikov, BNL-50727, Upton, NY, pp. 79-96 (1977).